

# Generalised Anderson coils for magnetic resonance imaging

F Momo<sup>†</sup>, O Adriani<sup>‡</sup>, G Gualtieri<sup>§</sup> and A Sotgiu<sup>§</sup>

<sup>†</sup> Dipartimento di Chimica-Fisica, Università di Venezia, Calle Larga Santa Marta, 30100 Venezia, Italy

<sup>‡</sup> Dipartimento di Medicina Interna, II Università di Roma, Tor Vergata, 00100 Roma, Italy

<sup>§</sup> Dipartimento di Scienze e Tecnologie Biomediche e di Biometria, Università dell'Aquila, Collemaggio, 67100 L'Aquila, Italy

Received 15 July 1987, in final form 3 November 1987

**Abstract.** A new method for generating highly linear field gradients over a large region of space is described. The coil assembly consists of two sets of  $n$  equispaced current lines laid on parallel planes whose values can be individually controlled. Field expressions are developed in Chebyshev polynomials and individual current control permits the required field profile to be achieved. Comparison between gradients obtained using conventional Anderson coils and the present ones shows a great improvement in gradient linearity, particularly when a large fraction of the coil assembly is considered.

## 1. Introduction

In either nuclear or electronic magnetic spin resonance imaging, linear field gradients are required for signal spatial deconvolution. Gradient coils should generate a linear field over a large fraction of the assembly; this is because coil dimensions are necessarily limited by mechanical and power constrictions.

This paper describes a new method of generating field gradients by two symmetric sets of  $n$  equispaced current lines (figure 1). Coil currents are used as independent variables and, in principle, can be adjusted to generate any given field profile; however, for its practical importance in imaging experiments, the properties of the system have been tested on constant gradients of the form  $dB_z/dy$ . Results are compared

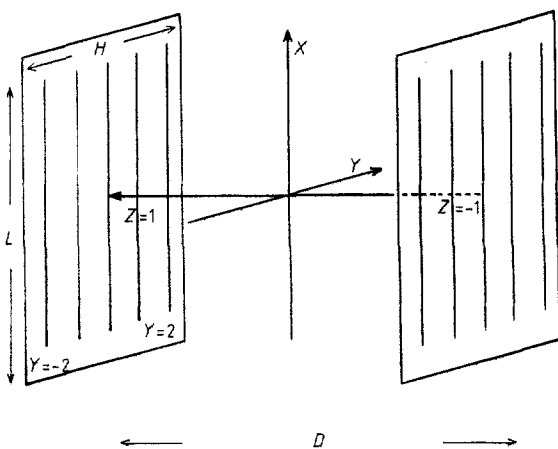


**Figure 1.** Reference system and view of a set of five equispaced current filaments. Distances are normalised following the convention used in the text.

with the usual Anderson coil configuration (Anderson 1961) used in the context of high resolution NMR spectroscopy. The better field linearity achievable over a large region is shown to be a consequence both of the field approximation used and of the larger number of current lines. Use of Chebyshev polynomials instead of expansion in spherical harmonics permits us to control the field shape over the full interval of definition of the polynomials.

Expansion in spherical harmonics, by contrast, gives a good fit only around the origin. This is a relevant point when the field profile must be controlled over a large fraction of the volume enclosed by the coil. In a recent paper Friedman *et al* (1984) approximate magnetic fields by a Legendre polynomials series using a least-squares technique over the whole region of interest. In the present case, we have chosen to fit  $B_z(y)$  by a polynomial expansion which minimises the integral of the generalised squares of errors, i.e.

$$I = \int_{-1}^1 w(y)(B_z(y) - a_0 Q_0(y) - a_1 Q_1(y) - \dots - a_m Q_m(y))^2 \quad (1)$$

where  $w(y)$  is a non-negative weighting function,  $Q_n(y)$  are  $n$ th degree polynomials,  $a_m$  are the coefficients of the expansion and the integral is defined on the interval  $(-1, 1)$ .

Chebyshev polynomials  $Q_k(y) = T_k(y) = \cos(k \cos^{-1} y)$  minimise equation (1) for  $w(y) = (1 - y^2)^{-1/2}$ . Their representation of the field  $B_z(y)$  has the properties that successive maximum errors alternate in sign and are approximately equal in absolute value (equal ripple property) and that the maximum error over a given interval is as small as possible.

## 2. Mathematical treatment and results

An infinitely long straight current line perpendicular to the  $YZ$  plane in the point  $(Y_0, Z_0)$  produces at  $(y, z)$  a field  $B_z$  given by:

$$B_z = \frac{\mu_0}{2\pi} I_x (y - Y_0) / [(y - Y_0)^2 + (z - Z_0)^2] \quad (2)$$

where  $I_x$  is the current value.

We will consider only the  $B_z$  component; in fact, in the context of magnetic resonances, when the strong magnetic field  $B_0$  is along the  $z$  axis, the contribution of the components  $B_x$  and  $B_y$  to the resonant frequency can be neglected. For practical purposes the model size has been normalised to the distance between current planes by fixing their positions at  $z = \pm Z_0 = \pm 1$ .

The  $n$  current filaments of the  $z = 1$  plane generate at the point  $(x, y)$  a field  $B_z$  given by

$$B_z = \frac{\mu_0}{2\pi} \sum_{j=1}^n P_j(y, z) I_j \quad (3)$$

where

$$P_j(y, z) = (y - Y_j) / [(y - Y_j)^2 + (z - Z_0)^2] \quad (4)$$

On the  $z = 0$  plane  $P_j(y, 0)$  can be approximated up to the  $m$ th term by (Abramovitz and Stegun 1970)

$$P_j(y, 0) = \sum_{k=1}^m a_{jk} T^k \quad (5)$$

where  $y$  belongs to the interval  $[-1, 1]$ . The coefficients  $a_{jk}$  which minimise equation (1) are:

$$a_{jk} = (2/N) = \sum_{i=1}^{N-1} P_j(y_i) T^k(y_i) \quad (6)$$

where

$$y_l = \cos[(2l + 1)\pi/2N]. \tag{7}$$

The total field  $B_z$  can be written as a sum of terms of the form  $A_j T^j(y)$ , i.e.

$$B_z(y, 0) = \frac{\mu_0}{2\pi} \sum_{j=1}^m A_j T^j(y) \tag{8}$$

where  $A_j$  are linear combinations of current values given by:

$$A_j = a_{1j} I_1 + a_{2j} I_2 + \dots + a_{nj} I_n. \tag{9}$$

An arbitrary field profile  $f(y)$  can be reproduced by equating each  $A_j$  to the corresponding coefficient of the Chebyshev expansion of  $f(y)$ . A linear system is then generated in the unknown  $I_i$ , which can be solved if  $m = n$ . The accuracy of the fitting and, in the present case, the linearity of the field are determined by the number of current filaments.

Having normalised to one the distance between the current planes, the separation between external wires is the only parameter that must be empirically fixed. Figure 5 shows that the amplitude of field fluctuations for sets of different numbers of current filaments presents a minimum when the distance  $H$  between the outermost filaments is about twice the plane separation  $D$ . For this reason  $H$  has been taken equal to  $2D$ .

The magnetic field profile generated at the plane  $z = 0$  by set of five filaments is shown in figure 2 and compared with the field produced by Anderson coils. Over the whole interval of definition of the Chebyshev expansion (i.e. from  $y = -1$  to  $y = 1$ , a length equal to coil spacing) the field fitting has a good accuracy, while, in case of Anderson coils, the linearity falls toward the extremes.

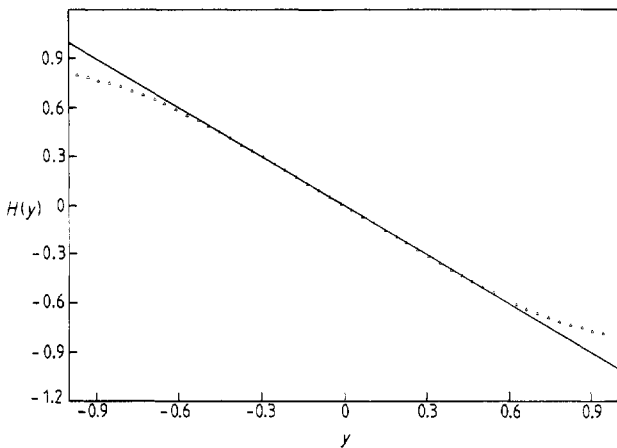


Figure 2. Full curve, field produced by a set of five equispaced coils along the  $y$  axis; triangles, field produced by a set of Anderson coils.

Figure 3(a) compares the linearity achieved by systems of 9, 7 and 5 filaments and Anderson coils; a magnified view of field fluctuations is shown in figure 3(b).

It must be observed that the Chebyshev expansion of the magnetic field  $B_z(y, z)$  has been performed on the function  $B_z(y, 0)$ , i.e. limited to the plane  $z = 0$ , and, in principle, nothing can be said on the field out of this plane. However numerical analysis (figure 4) shows that the field profile of the plane  $z = 0$  is maintained, with a good accuracy, on parallel planes at increasing distance from the origin.

### 3. Experiment

Practical design requires further considerations on physical dimensions of current filaments, which, in the previous math-

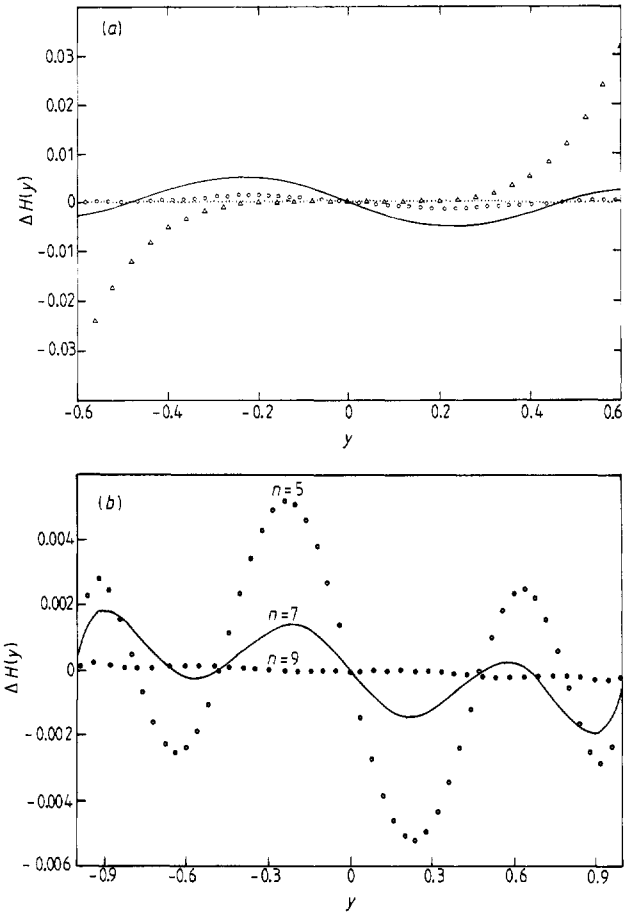


Figure 3. (a) Comparison between the linearity of fields produced by Anderson coils ( $\Delta$ ) and a set of five ( $\text{---}$ ), seven ( $\circ$ ) and nine ( $\cdots$ ) equispaced wires. (b) Enlarged view of field fluctuations along the  $y$  axis.  $\Delta H(y) = G(y - H(y))$ .

ematical description, were assumed of infinite length and dimensionless.

The case of finite length can be solved using the same procedure and substituting for equation (2) the correct field expression that for filaments extending from  $x = x_1$  to  $x = x_2$  is:

$$B_z = \frac{\mu_0}{4\pi} I_x (y - Y_0) \left\{ \frac{1}{[(y - Y_0)^2 + (z - Z_0)^2]} \times \{ (x - x_1) [(y - Y_0)^2 + (z - Z_0)^2 + (x - x_1)^2] + (x - x_2) [(y - Y_0)^2 + (z - Z_0)^2 + (x - x_2)^2] \} \right\}. \tag{10}$$

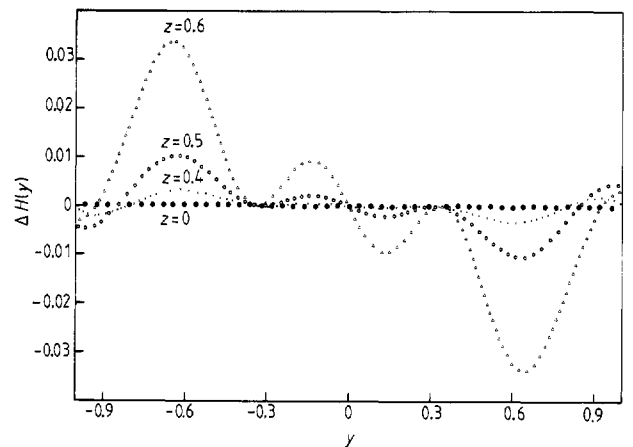


Figure 4. Field fluctuations for a set of nine equispaced filaments calculated in the  $y$  direction at various planes, i.e. at  $z = 0, 0.4, 0.5, 0.6$ .

Current sets of finite length should produce along the  $y$  axis or near to it an essentially linear gradient field. The effect of the finite length becomes increasingly important only outside this axis. This is shown in table 1 which gives field non-linearity in a cubic region of unit size centred on the

**Table 1.** Maximum field deviation times  $10^2$  for a unit gradient.  $x, y, z$  in normalised units;  $y$  ranging from  $-0.5$  to  $0.5$ . Top line: results for seven current filaments of infinite length; the rest of the table gives results of finite length filaments (extending from  $x = -2Z_0$  to  $2Z_0$ ).

$x$	$z$					
	0	0.1	0.2	0.3	0.4	0.5
0	0.12	0.16	0.30	0.63	1.41	3.20
0.1	0.13	0.20	0.42	0.92	1.98	4.27
0.2	0.12	0.18	0.40	0.90	1.96	4.25
0.3	0.26	0.24	0.34	0.84	1.90	4.19
0.4	0.51	0.49	0.44	0.74	1.80	4.09
0.5	0.85	0.83	0.79	0.79	1.65	3.94
0.5	1.30	1.28	1.24	1.24	1.47	3.75

origin. The use of normalised spatial coordinates implies that the gradient and magnetic fields should also be expressed in normalised form. The assumed magnetic field unit is the arbitrary field value at coordinates  $(0,1,0)$  (consistency with the arbitrary units of figures 2-5 is maintained). Table entries give the maximum field deviation along a straight line between  $y = -0.5$  and  $y = 0.5$ , for an array of points of the  $XZ$  plane. They have been obtained for infinite length current filaments and for filaments extending from  $x_1 = -2Z_0$  to  $x_2 = 2Z_0$ . In the considered volume maximum field deviation is mostly affected by displacements along the  $z$  direction

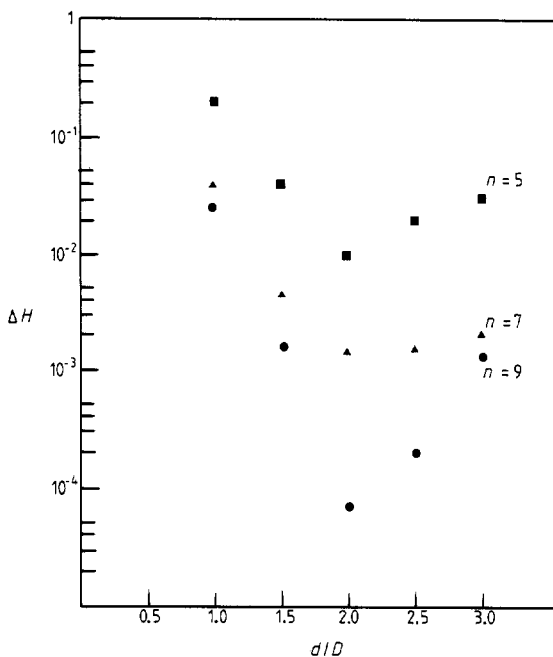


**Figure 5.** Maximum amplitude of field fluctuations (calculated along the  $y$  axis) for various sets of filaments. The tree plots are relative to systems of five, seven and nine filaments while the  $x$  axis gives the relative separation between the two outermost wires.  $D$  = separation between the planes;  $d$  = separation between the external coils on each plane.

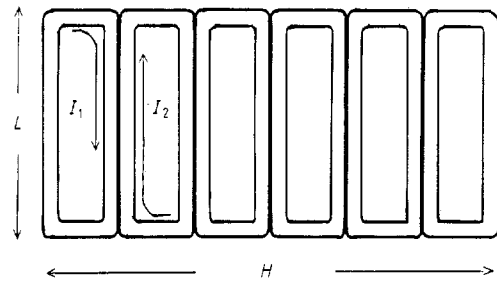


**Figure 6.** Sketch of the experimental assembly. One coil plane is shown.

( $3.20 \times 10^{-2}$  in normalised units for a unit gradient). The finite length of current filaments brings this value to  $4.25 \times 10^{-2}$ .

Use of dimensionless straight line wires is useful for illustrative purposes and is valid for very thin windings. However, the mathematical treatment previously shown is valid for any shape of the winding provided there is a linear dependence between field and currents.

A practical prototype consisting of six adjacent coils has been realised to provide field gradients in an ESR imaging experiment: this is illustrated in figure 6. The distance  $D$  between the planes on which the two sets are laid is 60 mm and consequently  $H = 120$  mm. Each coil is made of 100 turns of copper wire and has a square section  $5 \times 5$  mm<sup>2</sup> in size. In view of the results of table 1 the total coil length  $L$  has been set to 120 mm.

The expression for the field of each rectangular coil can be approximated by the field  $B_z(y, z)$  produced by two straight wires of finite thickness at a distance  $d$  apart and reversed currents. For a rectangular coil  $B_z$  is:

$$B_z(y, z) = \frac{\mu_0}{2\pi} j_x \int_{y_1}^{y_2} \left( \int_{z_1}^{z_2} (Y-y)/[(Y-y)^2 + (Z-z)^2] dZ - \int_{z_1+d}^{z_2+d} (Y-y)/[(Y-y)^2 + (Z-z)^2] dZ \right) dY. \quad (11)$$

More accurate values are obtained by integrating the expression for  $B_z$  given in equation (10). Both integrals have an exact solution and the  $B_z$  values give the coefficients  $P_j(y_i)$  of equation (6). Applying the previously outlined procedure to achieve a unitary constant gradient field ( $A_1 = 1, A_j = 0$  for  $j = 2, \dots, 6$ ) the six coil currents come out to be proportional to the numbers 12.337, 5.0603, 1.9964,  $-1.9964$ , 5.0603, 12.337. The multiplicative factor is a function of the number of turns and of the required gradient. For coils of 100 turns and for a gradient of  $0.1 \text{ T m}^{-1}$  this value is 0.45.

Deviation from linearity is given in table 2 which also makes a comparison with Anderson coils of the same dimensions. Measured field distribution obtained by this assembly is

**Table 2.** Maximum field deviation ( $\times 10^{-4} \text{ T}$ ) for a gradient of  $0.1 \text{ T m}^{-1}$ .

	$z$ (mm)					
	0	3	6	9	12	15
Present assembly	0.05	0.06	0.11	0.23	0.49	1.1
Anderson coils	0.4	0.3	0.17	0.6	1.44	2.6

shown in table 3. The values have been obtained by a gaussmeter which utilises a Hall probe as sensing device giving an accuracy of 0.1%.

To test the effect of current fluctuations on field homogeneity we repeatedly introduced in the current of each coil an independent random error up to the 0.1% of the total coil current. The resulting values of maximum field deviation at  $z = 0$  had a mean value of 0.051 with RMS 0.0076; this must be compared with the value of 0.05 reported in table 2 which represents the ripple of the Chebyshev approximation at the same position.

**Table 3.** Measured field (in  $10^{-4}$  T) on the plane  $X = 0$ .  $y$  and  $z$  are expressed in mm.

z	y						
	9	6	3	0	-3	-6	-9
9	-9.04	-6.04	-3.03	0.01	3.02	6.03	9.03
6	-9.04	6.03	3.03	0.00	3.00	6.01	9.02
3	-9.04	-6.03	-3.03	0.00	2.99	5.99	9.02
0	-9.00	-5.98	-3.00	0.00	3.01	6.02	9.01
-3	-8.97	-5.99	-2.99	0.00	3.02	6.01	9.02
-6	-9.03	-6.03	-3.02	0.01	3.02	6.02	9.03
-9	-9.04	-6.04	-3.02	0.01	3.03	6.03	9.04

In the present case the right current values are numerically generated by a personal computer interfaced with six independent 12-bit digital-to-analogue converters which drive the power output stages. Software control also allows the correction of DC offset errors of the current generators.

#### 4. Conclusions

Using the equal-ripple (or min-max error) properties of Chebyshev polynomials, it is possible to fit a given magnetic field profile with an accuracy that over a large volume is better than that obtained by the spherical harmonics expansion. It is obvious that these results have been achieved at the price of an increased number of coils. One merit of the proposed method is its capability of handling a high number of field-controlling variables (the  $n$  independent currents) by means of a set of linear equations.

#### References

- Abramovitz M and Stegun I A 1970 *Handbook of Mathematical Functions* (New York: Dover)
- Anderson W A 1961 Electrical current shims for correcting magnetic fields *Rev. Sci. Instrum.* **32** 241
- Friedman M, Avida R, Brandstadter J and Erez G 1984 Homogeneous magnetic field in a cylindrical shell *J. Phys. E: Sci. Instrum.* **17** 212

## A novel Kerr cell

K Kikuchi, G Honda and H Watanabe

Department of Chemistry, College of Arts and Sciences, The University of Tokyo, Komaba, Meguro-ku, Tokyo 153, Japan

Received 14 September 1987, in final form 16 November 1987

**Abstract.** A method of fixing the metal electrodes simplified the structure of an electric birefringence cell. A Kerr cell of optical path length 57 mm and electrode separation 3 mm was constructed. The electrodes are tightly fastened by a simple means using no glues and spacers. The residual birefringence of the cell windows is negligible. The overall structure is so simple and firm that it is possible to surround the sample compartment with a temperature jacket more closely than in any other previous Kerr cell design. It is mounted free from vibrations of the circulation pump and is able to sustain field strengths of several  $\text{MV m}^{-1}$ . Filling and emptying the sample compartment are easy.

#### 1. Introduction

Molecules in solution possessing electrical and optical anisotropies respond to an applied electric field by orientation and macroscopic optical anisotropies are induced. Among other electro-optic effects, electric birefringence (the Kerr effect) has been of widespread use for molecular characterisation because of its high sensitivity (Yoshioka and Watanabe 1969, Fredericq and Houssier 1973, O'Konski 1976, Jennings 1979, Krause 1981). Measurement of the amplitude and temporal response of the transient electric birefringence provides information about the electrical, optical and hydrodynamic properties of molecules.

While recent advances in instrumentation have been exploited to refine the technique, defects in the early Kerr cell designs (O'Konski and Haltner 1956, Shah *et al* 1963, Ikeda *et al* 1965, Fredericq and Houssier 1973) have been appreciated and many alternatives proposed (Orttung and Meyers 1963, Jerrard *et al* 1969, Bernengo *et al* 1973, Baily 1975, Coles 1977, Lewis and Orttung 1978, Khanna *et al* 1978, Elias and Eden 1981, Wijmenga *et al* 1985). In all these new cells special care has been exercised in the attachment of windows to the cell body to reduce the residual birefringence, i.e. an optical retardation due to the strain birefringence in the windows, often occurring in the absence of an electric field. For example, one of the problems in the early cell designs which used commercially available spectrophotometer cuvettes is that their end windows are not free from strain, leading to a large residual birefringence in the optical system.

Recently an elaborate Kerr cell design has been proposed by Wijmenga *et al* (1985). They devised a special adjustable low-strain attachment of Suprasil windows to the cell body thereby reducing the residual retardation below a few minutes (they are the first Kerr cell manufacturers who stated the magnitude of the retardation explicitly). The platinum electrodes are fastened parallel with complete precision and the lead wires from them are ingeniously insulated from the surrounding water jacket. Every joint position is sealed by an